Science Advances
AAAS

Supplementary Materials for

Continuous rise of the tropopause in the Northern Hemisphere over 1980–2020

Lingyun Meng, Jane Liu*, David W. Tarasick, William J. Randel*, Andrea K. Steiner, Hallgeir Wilhelmsen, Lei Wang, Leopold Haimberger

*Corresponding author. Email: janejj.liu@utoronto.ca (J.L.); randel@ucar.edu (W.J.R.)

Published 5 November 2021, *Sci. Adv.* **7**, eabi8065 (2021)
DOI: 10.1126/sciadv.abi8065

This PDF file includes:

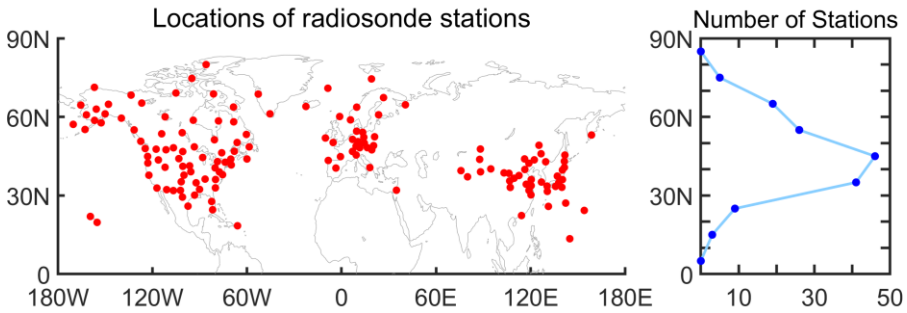

Fig. S1. Distribution of the radiosonde stations. Locations of the radiosonde stations used in this study and the number of stations in each 10° latitudinal band.

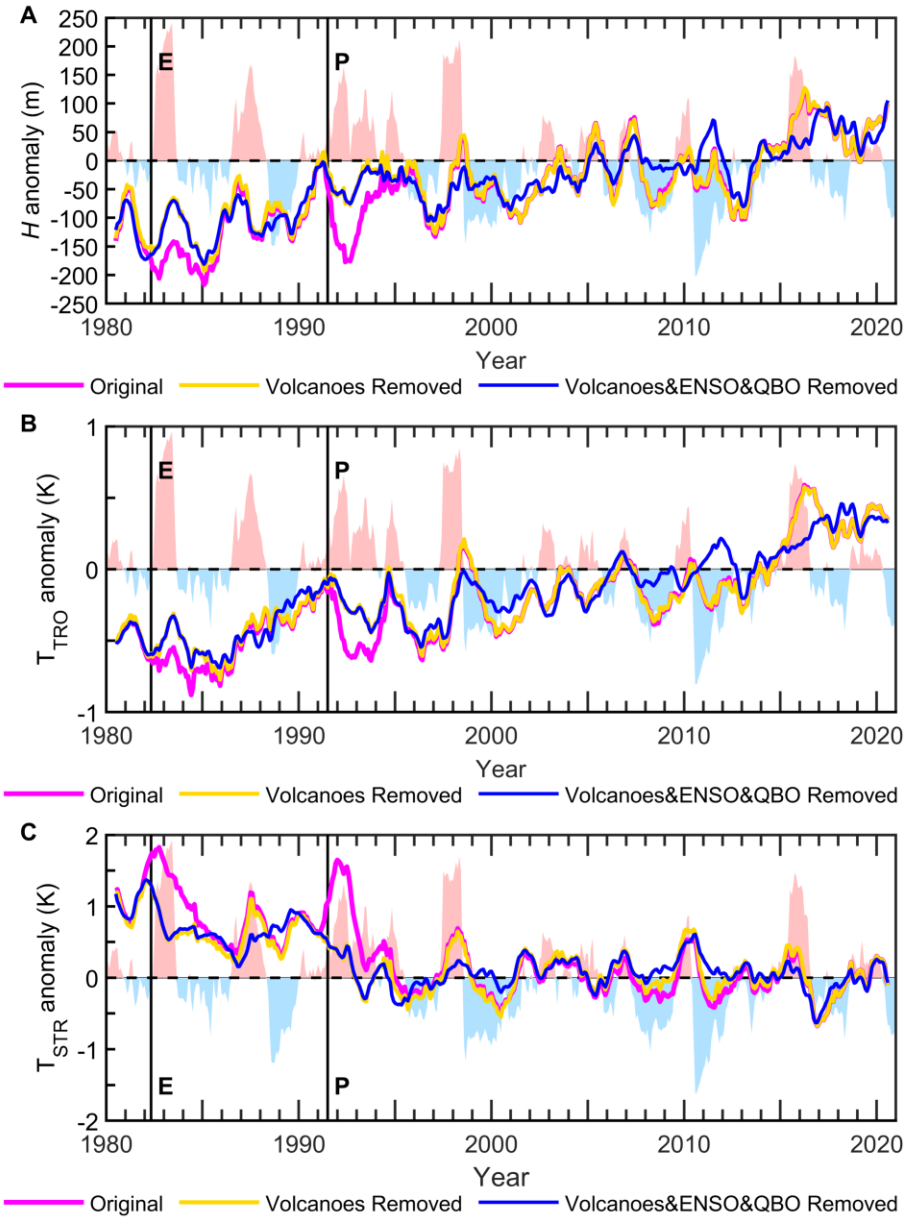

Fig. S2. The original and natural variability-removed time series of *H*, T_{TRO}, and T_{STR} in the IGRA2 radiosonde data. Time series of the 11-month running mean of monthly anomalies of *H* **(A)**, T_{TRO} **(B)**, and T_{STR} **(C)** in the original time series (pink line), as well as in the volcanic-effect-removed (yellow line), and volcanic-ENSO-QBO-effect-removed (blue line) time series in the Northern Hemisphere over 20°N to 80°N from 1980 to 2020. The two vertical black lines respectively indicate the large volcanic eruptions of El Chichón (April 1982) and Mount Pinatubo (June 1991). The shaded areas indicate the variations in the ENSO index over 1980-2020 with negative phases in light blue and positive phases in light pink. Note that the atmospheric response is lagging the ENSO index by about three months (*53, 58, 67*).

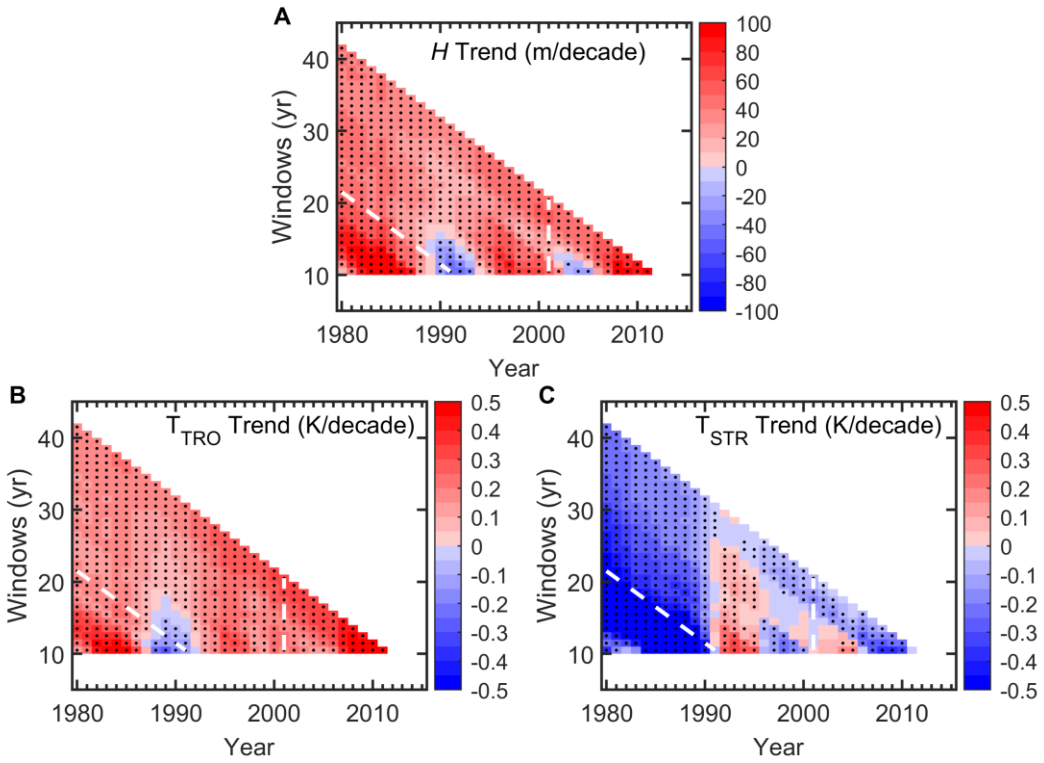

Fig. S3. Running windows for linear trends in *H* (A), T_{TRO} (B), and T_{STR} (C) over 1980-2020 in the IGRA2 radiosonde data. The *x*-axis indicates the start year, and the *y*-axis indicates the number of years since the start year. The inclined white line indicates all linear trends ending in 2000, while the vertical white line indicates all linear trends starting in 2001. Trends that are statistically significant at the 95% confidence level are indicated by black dots. Note that running windows with lengths less than 10 years are not considered and thus not shown.

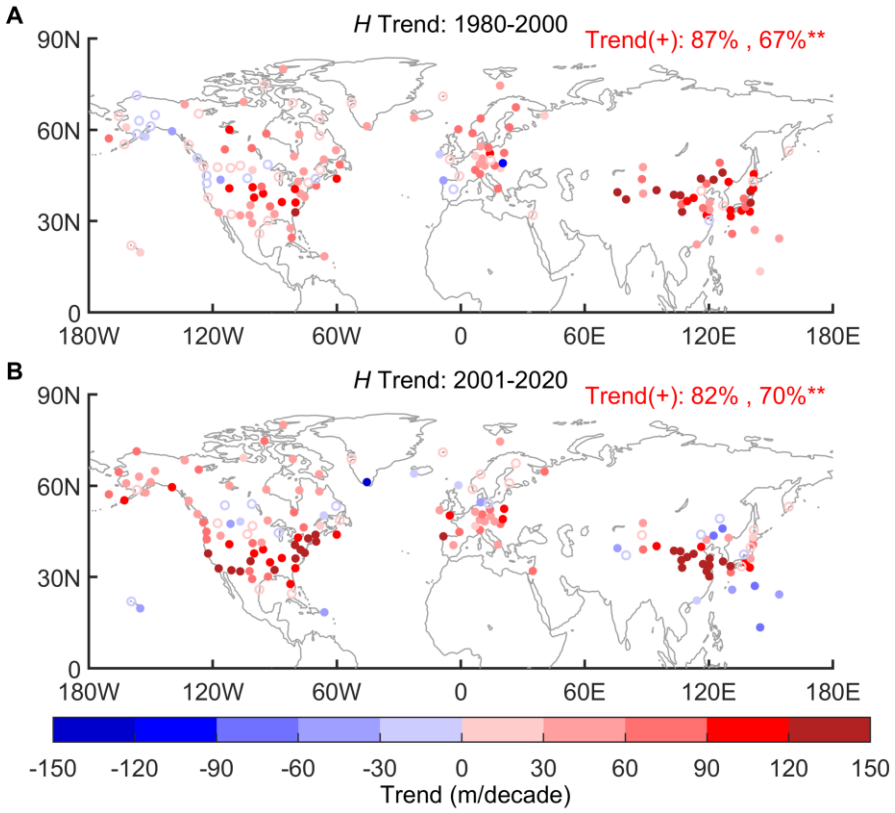

Fig. S4. The spatial distribution of the trend in *H* over 1980-2000 (A) and 2001-2020 (B) in the IGRA2 radiosonde data. Dots (circles) indicate statistically significant (insignificant) trends at the 95% confidence level. The red numbers in (A) and (B) indicate the percentage of stations with positive trends and with significant positive trends at the 95% confidence level indicated by double asterisks.

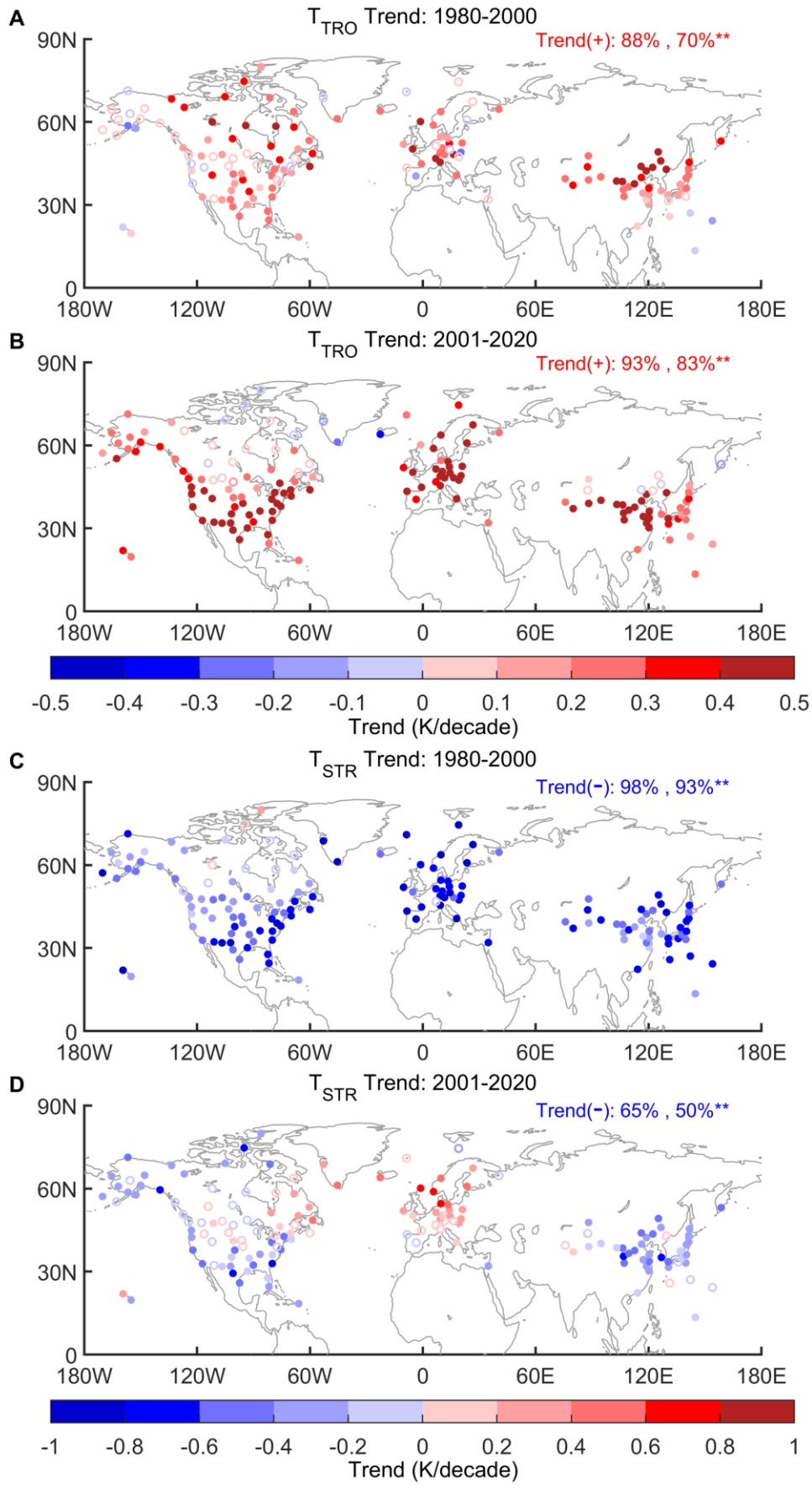
A
T TRO Trend: 1980-2000
Trend(+): 88% , 70%**
B
T TRO Trend: 2001-2020
Trend(+): 93% , 83%**
90N
60N
30N
0
180W
120W
60W
0
60E
120E
180E
-0.5
-0.4
-0.3
-0.2
-0.1
0
0.1
0.2
0.3
0.4
0.5
Trend (K/decade)
C
T STR Trend: 1980-2000
Trend(-): 98% , 93%**
D
T STR Trend: 2001-2020
Trend(-): 65% , 50%**
-1
-0.8
-0.6
-0.4
-0.2
0
0.2
0.4
0.6
0.8
1
Trend (K/decade)

Fig. S5. The spatial distribution of the trend in T_{TRO} (A and B) and T_{STR} (C and D) over 1980-2000 and 2001-2020 in the IGRA2 radiosonde data. Dots (circles) indicate statistically significant (insignificant) trends at the 95% confidence level. The numbers in red (blue) in a subplot indicate the percentage of stations with positive (negative) trends, and with significant positive (negative) trends at the 95% confidence level indicated by double asterisks.

Table S1. Information on the radiosonde stations selected for this study. The information includes latitude, longitude, the World Meteorological Organization Identification Number (ID), country, and the total number of missing monthly data of tropopause height over 1980-2020.

Station	Latitude	Longitude	ID	Country	Missing Data
WEATHER FORECAST OFFICE	13.48	144.79	91212	GQ	44
PR SAN JUAN/INT.	18.43	-65.99	78526	RQ	15
HI HILO HI	19.72	-155.06	91285	US	8
HI LIHUE	21.99	-159.35	91165	US	11
KOWLOON	22.33	114.17	45004	HK	25
MINAMITORISHIMA	24.29	153.98	47991	JA	35
FL KEY WEST/INT.	24.55	-81.79	72201	US	37
MINAMIDAITOJIMA	25.83	131.23	47945	JA	48
TX BROWNSVILLE/INT.	25.92	-97.42	72250	US	26
CHICHIJIMA	27.09	142.19	47971	JA	50
FL TAMPA BAY AREA	27.71	-82.4	72210	US	10
TX DEL RIO/INT.	29.37	-100.92	72261	US	2
LA LAKE CHARLES/MUN.	30.13	-93.22	72240	US	8
HANGZHOU	30.23	120.17	58457	CH	61
KAGOSHIMA	31.56	130.55	47827	JA	31
TX SANTA TERESA	31.87	-106.7	72364	US	5
NANJING	31.93	118.9	58238	CH	26
TX MIDLAND/MIDLAND REG. AIRTERM	31.94	-102.19	72265	US	4
BET DAGAN	32	34.82	40179	IS	33
AZ TUCSON	32.23	-110.96	72274	US	3
MS JACKSON/ALLEN C. THOMPSON FIEL	32.32	-90.08	72235	US	2
CA SAN DIEGO/MIRAMAR	32.83	-117.12	72293	US	1
SC CHARLESTON/MUN.	32.9	-80.03	72208	US	11
HANZHONG	33.07	107.03	57127	CH	39
HACHIJOJIMA	33.12	139.78	47678	JA	24
SHIONOMISAKI	33.45	135.76	47778	JA	25
FUKUOKA	33.58	130.38	47807	JA	6
SHEYANG	33.75	120.3	58150	CH	23
XUZHOU	34.28	117.15	58027	CH	28
HAMAMATSU AB	34.75	137.7	47681	JA	25
AR LITTLE ROCK/ADAMS FLD	34.84	-92.26	72340	US	0
GWANGJU AB	35.12	126.8	47158	KS	20
TX AMARILLO/INTL.	35.23	-101.71	72363	US	2
PINGLIANG	35.55	106.67	53915	CH	20
TATENO	36.06	140.13	47646	JA	6
QINGDAO	36.07	120.33	54857	CH	25
NC GREENSBORO/G.-HIGH PT.	36.1	-79.94	72317	US	4
TN NASHVILLE/OLD HICKORY	36.25	-86.56	72327	US	1
YAN AN	36.57	109.45	53845	CH	20
HOTAN	37.13	79.93	51828	CH	21
WAJIMA	37.39	136.9	47600	JA	7
TAIYUAN	37.62	112.58	53772	CH	22
CA OAKLAND/METROP. OAKLAND INT.	37.74	-122.22	72493	US	3
KS DODGE CITY/MUN.	37.76	-99.97	72451	US	0
VA WALLOPS ISLAND	37.93	-75.48	72402	US	17
YINCHUAN	38.47	106.2	53614	CH	17
MINQIN	38.63	103.08	52681	CH	21
VA STERLING	38.98	-77.49	72403	US	7
RUOQIANG	39.03	88.17	51777	CH	21
KS TOPEKA/MUN.	39.07	-95.63	72456	US	0
KASHI	39.48	75.75	51709	CH	25
AKITA	39.72	140.1	47582	JA	4
BEIJING	39.93	116.28	54511	CH	38
DUNHUANG	40.15	94.68	52418	CH	19
MADRID/BARAJAS RS	40.47	-3.58	8221	SP	24
PA PITTSBURGH	40.53	-80.22	72520	US	2
BRINDISI RDS	40.66	17.96	16320	IT	55

MISAWA AB	40.71	141.37	47580	JA	13
UT SALT LAKE CITY/INTNL UT.	40.77	-111.96	72572	US	4
NE NORTH PLATTE/LEE BIRD	41.13	-100.7	72562	US	1
NE VALLEY	41.32	-96.37	72558	US	3
MA CHATHAM	41.66	-69.96	74494	US	6
CHIFENG	42.3	118.83	54218	CH	63
OR MEDFORD/MEDFORD-JACKSON COUNTY	42.38	-122.88	72597	US	1
NY ALBANY	42.69	-73.83	72518	US	5
YANJI	42.87	129.5	54292	CH	60
NY BUFFALO/GREATER BUFFALO INT.	42.94	-78.72	72528	US	0
SAPPORO	43.06	141.33	47412	JA	19
LA CORUNA	43.37	-8.42	8001	SP	33
ID BOISE/MUN.	43.57	-116.21	72681	US	5
TONGLIAO	43.6	122.27	54135	CH	48
WU LU MU QI	43.78	87.62	51463	CH	57
ME GRAY	43.89	-70.26	74389	US	0
SABLE ISLAND	43.93	-60.01	71600	CA	24
XILIN HOT	43.95	116.12	54102	CH	40
SD RAPID CITY WFO	44.07	-103.21	72662	US	5
WI GREEN BAY/A.-STRAUBEL	44.5	-88.11	72645	US	8
BORDEAUX MERIGNAC	44.83	-0.69	7510	FR	14
OR SALEM/MCNARY	44.91	-123.01	72694	US	3
WAKKANAI	45.42	141.68	47401	JA	10
MILANO LINATE RDS	45.46	9.28	16080	IT	4
HARBIN	45.93	126.57	50953	CH	30
MANIWAKI UA	46.3	-76.01	71722	CA	3
ND BISMARCK/MUN.	46.77	-100.76	72764	US	8
PAYERNE	46.81	6.94	6610	SZ	20
ME CARIBOU/MUN.	46.87	-68.01	72712	US	0
BUDAPEST/PESTSZENTLORINC	47.43	19.18	12843	HU	37
MT GREAT FALLS	47.46	-111.38	72776	US	1
WA SPOKANE	47.68	-117.63	72786	US	3
ALTAY	47.73	88.08	51076	CH	15
WA QUILLAYUTE	47.93	-124.56	72797	US	4
MT GLASGOW/INT.	48.21	-106.63	72768	US	4
MUENCHEN-OBERSCHLEISSHEIM	48.24	11.55	10868	GM	3
WIEN/HOHE WARTE	48.25	16.36	11035	AU	24
MN INT.FALLS/FALLS INT. MN.	48.56	-93.4	72747	US	7
STEPHENVILLE UA	48.57	-58.57	71815	CA	47
STUTTGART/SCHNARRENBERG	48.83	9.2	10739	GM	4
POPRAD-GANOVCE	49.03	20.32	11952	LO	7
NENJIANG	49.17	125.23	50557	CH	26
PRAHA-LIBUS	50.01	14.45	11520	EZ	4
CAMBORNE	50.22	-5.33	3808	UK	9
SEPT-ILES UA	50.22	-66.25	71811	CA	3
MEININGEN	50.56	10.38	10548	GM	3
PORT HARDY UA	50.69	-127.38	71109	CA	11
MOOSONEE UA	51.27	-80.65	71836	CA	20
ESSEN-BREDENEY	51.41	6.97	10410	GM	3
VALENTIA OBSERVATORY	51.94	-10.24	3953	EI	15
LINDENBERG	52.22	14.12	10393	GM	3
LEGIONOWO	52.41	20.96	12374	PL	9
PETROPAVLOVSK-KAMCHATSKIJ	53.08	158.58	32540	RS	42
GOOSE UA	53.3	-60.37	71816	CA	7
EDMONTON STONY PLAIN	53.55	-114.11	71119	CA	3
THE PAS UA	53.97	-101.1	71867	CA	3
GREIFSWALD	54.1	13.41	10184	GM	5
SCHLESWIG	54.53	9.55	10035	GM	19
AK ANNETTE ISLAND	55.04	-131.58	70398	US	11
AK COLD BAY	55.2	-162.72	70316	US	12
AK ST. PAUL ISLANDS	57.15	-170.22	70308	US	22
AK KODIAK	57.74	-152.49	70350	US	1
KUUJJUAQ	58.12	-68.42	71906	CA	9
INUKJUAK UA	58.47	-78.08	71907	CA	12
AK KING SALMON	58.68	-156.67	70326	US	10
CHURCHILL A UA	58.73	-94.07	71913	CA	21

STAVANGER/SOLA	58.87	5.67	1415	NO	13
AK YAKUTAT	59.52	-139.67	70361	US	8
FORT SMITH UA	60.03	-111.93	71934	CA	6
LERWICK	60.14	-1.18	3005	UK	24
AK BETHEL/BETHEL AIRPORT	60.79	-161.84	70219	US	11
JOKIOINEN OBSERVATORY	60.81	23.5	2963	FI	12
AK ANCHORAGE/INT.	61.16	-149.99	70273	US	0
MITTARFIK NARSARSUAQ	61.17	-45.42	4270	GL	11
AK MCGRATH	62.96	-155.6	70231	US	26
ORLAND III	63.71	9.61	1241	NO	31
IQALUIT UA	63.75	-68.55	71909	CA	9
KEFLAVIKURFLUGVOLLUR	63.98	-22.6	4018	IC	15
AK NOME	64.51	-165.43	70200	US	8
ARHANGEL SK	64.62	40.51	22543	RS	34
AK FAIRBANKS/INT.	64.82	-147.88	70261	US	0
NORMAN WELLS UA	65.28	-126.75	71043	CA	8
SODANKYLA ARCTIC RESEARCH CENT	67.37	26.63	2836	FI	8
INUVIK UA	68.32	-133.52	71957	CA	4
AASIAAT (EGEDESMINDE)	68.71	-52.85	4220	GL	23
HALL BEACH UA	68.77	-81.22	71081	CA	5
CAMBRIDGE BAY UA	69.13	-105.07	71925	CA	1
JAN MAYEN	70.94	-8.67	1001	JN	22
AK BARROW/W. POST W. ROGERS	71.29	-156.78	70026	US	23
BJORNOYA	74.5	19	1028	SV	9
RESOLUTE UA	74.7	-94.97	71924	CA	5
EUREKA UA	79.98	-85.93	71917	CA	3

Table S2. The correlations between trends of H and of T_{TRO} and between trends of H and of T_{STR}. The correlation coefficients (r) between trends of H and of T_{TRO} and of T_{STR} in the Northern Hemisphere (20°N to 80°N) over 1980-2000 and 2001-2020. The corresponding regression coefficients are also shown.

Correlation	**1980-2000**	**2001-2020**
	Correlation coefficient	
r (H_{Trend}, T_{TRO_Trend})	0.61	0.66
r (H_{Trend}, T_{STR_Trend})	-0.19	-0.37
	Regression coefficient (m/K)	
δH_{Trend} / δT_{TRO_Trend}	191.1	173.1
δH_{Trend} / δT_{STR_Trend}	-54.0	-99.9

REFERENCES AND NOTES

1. A. C. Boothe, C. R. Homeyer, Global large-scale stratosphere-troposphere exchange in modern reanalyses. *Atmos. Chem. Phys.* **17**, 5537–5559 (2017).

2. J. R. Holton, P. H. Haynes, M. E. McIntyre, A. R. Douglass, R. B. Rood, L. Pfister, Stratosphere-troposphere exchange. *Rev. Geophys.* **33**, 403–439 (1995).

3. W. J. Randel, D. J. Seidel, L. L. Pan, Observational characteristics of double tropopauses. *J. Geophys. Res.* **112**, D07309 (2007).

4. B. D. Santer, M. F. Wehner, T. M. L. Wigley, R. Sausen, G. A. Meehl, K. E. Taylor, C. Ammann, J. Arblaster, W. M. Washington, J. S. Boyle, W. Bruggemann, Contributions of anthropogenic and natural forcing to recent tropopause height changes. *Science* **301**, 479–483 (2003).

5. D. J. Seidel, W. J. Randel, Variability and trends in the global tropopause estimated from radiosonde data. *J. Geophys. Res.* **111**, D21101 (2006).

6. D. J. Seidel, R. J. Ross, J. K. Angell, G. C. Reid, Climatological characteristics of the tropical tropopause as revealed by radiosondes. *J. Geophys. Res.* **106**, 7857–7878 (2001).

7. B. D. Santer, R. Sausen, T. M. L. Wigley, J. S. Boyle, K. AchutaRao, C. Doutriaux, J. E. Hansen, G. A. Meehl, E. Roeckner, R. Ruedy, G. Schmidt, K. E. Taylor, Behavior of tropopause height and atmospheric temperature in models, reanalyses, and observations: Decadal changes. *J. Geophys. Res.* **108**, ACL 1-1–ACL 1-22 (2003).

8. B. D. Santer, T. M. L. Wigley, A. J. Simmons, P. W. Kallberg, G. A. Kelly, S. M. Uppala, C. Ammann, J. S. Boyle, W. Bruggemann, C. Doutriaux, M. Fiorino, C. Mears, G. A. Meehl, R. Sausen, K. E. Taylor, W. M. Washington, M. F. Wehner, F. J. Wentz, Identification of anthropogenic climate change using a second-generation reanalysis. *J. Geophys. Res.* **109**, D21104 (2004).

9. S.-W. Son, L. M. Polvani, D. W. Waugh, T. Birner, H. Akiyoshi, R. R. Garcia, A. Gettelman, D. A. Plummer, E. Rozanov, The impact of stratospheric ozone recovery on tropopause height trends. *J. Climate* **22**, 429–445 (2009).

10. A. C. Maycock, W. J. Randel, A. K. Steiner, A. Y. Karpechko, J. Christy, R. Saunders, D. W. J. Thompson, C.-Z. Zou, A. Chrysanthou, N. L. Abraham, H. Akiyoshi, A. T. Archibald, N. Butchart, M. Chipperfield, M. Dameris, M. Deushi, S. Dhomse, G. Di Genova, P. Joeckel, D. E. Kinnison, O. Kirner, F. Ladstädter, M. Michou, O. Morgenstern, F. O'Connor, L. Oman, G. Pitari, D. A. Plummer, L. E. Revell, E. Rozanov, A. Stenke, D. Visioni, Y. Yamashita, G. Zeng, Revisiting the mystery of recent stratospheric temperature trends. *Geophys. Res. Lett.* **45**, 9919–9933 (2018).

11. C. McLandress, T. G. Shepherd, A. I. Jonsson, T. von Clarmann, B. Funke, A method for merging nadir-sounding climate records, with an application to the global-mean stratospheric temperature data sets from SSU and AMSU. *Atmos. Chem. Phys.* **15**, 9271–9284 (2015).

12. R. Philipona, C. Mears, M. Fujiwara, P. Jeannet, P. Thorne, G. Bodeker, L. Haimberger, M. Hervo, C. Popp, G. Romanens, W. Steinbrecht, R. Stubi, R. Van Malderen, Radiosondes show that after decades of cooling, the lower stratosphere is now warming. *J. Geophys. Res. Atmos.* **123**, 12509–12522 (2018).

13. W. J. Randel, L. Polvani, F. Wu, D. E. Kinnison, C.-Z. Zou, C. Mears, Troposphere-stratosphere temperature trends derived from satellite data compared with ensemble simulations from WACCM. *J. Geophys. Res. Atmos.* **122**, 9651–9667 (2017).

14. A. K. Steiner, F. Ladstädter, W. J. Randel, A. C. Maycock, Q. Fu, C. Claud, H. Gleisner, L. Haimberger, S. -P. Ho, P. Keckhut, T. Leblanc, C. Mears, L. M. Polvani, B. D. Santer, T. Schmidt, V. Sofieva, R. Wing, C. -Z. Zou, Observed temperature changes in the troposphere and stratosphere from 1979 to 2018. *J. Climate* **33**, 8165–8194 (2020).

15. A. Dai, J. C. Fyfe, S.-P. Xie, X. Dai, Decadal modulation of global surface temperature by internal climate variability. *Nat. Clim. Chang.* **5**, 555–559 (2015).

16. J. C. Fyfe, G. A. Meehl, M. H. England, M. E. Mann, B. D. Santer, G. M. Flato, E. Hawkins, N. P. Gillett, S.-P. Xie, Y. Kosaka, N. C. Swart, Making sense of the early-2000s warming slowdown. *Nat. Clim. Chang.* **6**, 224–228 (2016).

17. H. Gleisner, P. Thejll, B. Christiansen, J. K. Nielsen, Recent global warming hiatus dominated by low-latitude temperature trends in surface and troposphere data. *Geophys. Res. Lett.* **42**, 510–517 (2015).

18. Y. Kosaka, S. -P. Xie, Recent global-warming hiatus tied to equatorial Pacific surface cooling. *Nature* **501**, 403–407 (2013).

19. L. Dong, M. J. McPhaden, The role of external forcing and internal variability in regulating global mean surface temperatures on decadal timescales. *Environ. Res. Lett.* **12**, 034011 (2017).

20. S. Hu, A. V. Fedorov, The extreme El Niño of 2015-2016 and the end of global warming hiatus. *Geophys. Res. Lett.* **44**, 3816–3824 (2017).

21. M. Shagngguan, W. Wang, S. Jin, Variability of temperature and ozone in the upper troposphere and lower stratosphere from multi-satellite observations and reanalysis data. *Atmos. Chem. Phys.* **19**, 6659–6679 (2019).

22. R. Sausen, B. D. Santer, Use of changes in tropopause height to detect human influences on climate. *Meteorol. Z.* **12**, 131–136 (2003).

23. P. Pisoft, P. Sacha, L. M. Polvani, J. A. Añel, L. de la Torre, R. Eichinger, U. Foelsche, P. Huszar, C. Jacobi, J. Karlicky, A. Kuchar, J. Miksovsky, M. Zak, H. E. Rieder, Stratospheric contraction caused by increasing greenhouse gases. *Environ. Res. Lett.* **16**, 064038 (2021).

24. I. Durre, R. S. Vose, X. Yin, S. Applequist, J. Arnfield, Integrated Global Radiosonde Archive (IGRA) version 2, NOAA/National Centers for Environmental Information, **10**, V5X63X0Q (2016); https://doi.org/10.7289/V5X63K0Q.

25. EOPAC Team, GNSS Radio Occultation Record (OPS 5.6 2001–2020), Wegener Center, University of Graz, Austria (2021); https://doi.org/10.25364/WEGC/OPS5.6:2021.1.

26. L. Haimberger, Homogenization of radiosonde temperature time series using innovation statistics. *J. Climate* **20**, 1377–1403 (2007).

27. L. Haimberger, C. Tavolato, S. Sperka, Homogenization of the global radiosonde temperature dataset through combined comparison with reanalysis background series and neighboring stations. *J. Climate* **25**, 8108–8131 (2012).

28. E. J. Highwood, B. J. Hoskins, P. Berrisford, Properties of the Arctic tropopause. *Q. J. R. Meteorol. Soc.* **126**, 1515–1532 (2000).

29. Q. Fu, C. M. Johanson, J. M. Wallace, T. Reichler, Enhanced mid-latitude tropospheric warming in satellite measurements. *Science* **312**, 1179 (2006).

30. D. J. Seidel, W. J. Randel, Recent widening of the tropical belt: Evidence from tropopause observations. *J. Geophys. Res.* **112**, D20113 (2007).

31. P. W. Staten, J. Lu, K. M. Grise, S. M. Davis, T. Birner, Re-examining tropical expansion. *Nat. Clim. Chang.* **8**, 768–775 (2018).

32. T. Schmidt, J. Wickert, G. Beyerle, S. Heise, Global tropopause height trends estimated from GPS radio occultation data. *Geophys. Res. Lett.* **35**, L11806 (2008).

33. B. J. Hoskins, M. E. McIntyre, A. W. Robertson, On the use and significance of isentropic potential vorticity maps. *Q. J. R. Meteorol. Soc.* **111**, 877–946 (1985).

34. B. Efron, Bootstrap methods: Another look at the jackknife. *Ann. Stat.* **7**, 1–26 (1979).

35. V. Aquila, W. H. Swartz, D. W. Waugh, P. R. Colarco, S. Pawson, L. M. Polvani, R. S. Stolarski, Isolating the roles of different forcing agents in global stratospheric temperature changes using model integrations with incrementally added single forcings. *J. Geophys. Res. Atmos.* **121**, 8067–8082 (2016).

36. J. Liu, D. W. Tarasick, V. E. Fioletov, C. McLinden, T. Zhao, S. Gong, C. Sioris, J. J. Jin, G. Liu, O. Moeini, A global ozone climatology from ozone soundings via trajectory mapping: A stratospheric perspective. *Atmos. Chem. Phys.* **13**, 11441–11464 (2013).

37. E. C. Weatherhead, S. B. Andersen, The search for signs of recovery of the ozone layer. *Nature* **441**, 39–45 (2006).

38. J. R. Ziemke, S. Chandra, Development of a climate record of tropospheric and stratospheric column ozone from satellite remote sensing: Evidence of an early recovery of global stratospheric ozone. *Atmos. Chem. Phys.* **12**, 5737–5753 (2012).

39. World Meteorological Organization (WMO), Executive Summary: Scientific assessment of ozone depletion: 2018, World Meteorological Organization, Global Ozone Research and Monitoring Project—Report No. 58, 67 pp., Geneva, Switzerland.

40. M. Weber, M. Coldewey-Egbers, V. E. Fioletov, S. M. Frith, J. D. Wild, J. P. Burrows, C. S. Long, D. Loyola, Total ozone trends from 1979 to 2016 derived from five merged observational datasets—The emergence into ozone recovery. *Atmos. Chem. Phys.* **18**, 2097–2117 (2018).

41. Y. Zhang, J. M. Wallace, D. S. Battisti, ENSO-like interdecadal variability: 1900-93. *J. Climate* **10**, 1004–1020 (1997).

42. I. Durre, R. S. Vose, D. B. Wuertz, Overview of the Integrated Global Radiosonde Archive. *J. Climate* **19**, 53–68 (2006).

43. World Meteorological Organization (WMO), Meteorology—A three-dimensional science: Second session of the Commission for Aerology [WMO Bulletin IV(4), WMO, Geneva, 1957], pp. 134–138.

44. G. Zängl, K. P. Hoinka, The tropopause in the polar regions. *J. Climate* **14**, 3117–3139 (2001).

45. S. M. Uppala, P. W. Kållberg, A. J. Simmons, U. Andrae, V. Da Costa Bechtold, M. Fiorino, J. K. Gibson, J. Haseler, A. Hernandez, G. A. Kelly, X. Li, K. Onogi, S. Saarinen, N. Sokka, R. P. Allan, E. Andersson, K. Arpe, M. A. Balmaseda, A. C. M. Beljaars, L. Van De Berg, J. Bidlot, N. Bormann, S. Caires, F. Chevallier, A. Dethof, M. Dragosavac, M. Fisher, M. Fuentes, S. Hagemann, E. Hólm, B. J. Hoskins, L. Isaksen, P. A. E. M. Janssen, R. Jenne, A. P. McNally, J.-F. Mahfouf, J.-J. Morcrette, N. A. Rayner, R. W. Saunders, P. Simon, A. Sterl, K. E. Trenberth, A. Untch, D. Vasiljevic, P. Viterbo, J. Woollen, The ERA-40 re-analysis. *Q. J. R. Meteorol. Soc.* **131**, 2961–3012 (2005).

46. D. P. Dee, S. M. Uppala, A. J. Simmons, P. Berrisford, P. Poli, S. Kobayashi, U. Andrae, M. A. Balmaseda, G. Balsamo, P. Bauer, P. Bechtold, A. C. M. Beljaars, L. van de Berg, J. Bidlot, N. Bormann, C. Delsol, R. Dragani, M. Fuentes, A. J. Geer, L. Haimberger, S. B. Healy, H. Hersbach, E. Hólm, L. Isaksen, P. Kållberg, M. Köhler, M. Matricardi, A. P. McNally, B. M. Monge-Sanz, J.-J. Morcrette, B.-K. Park, C. Peubey, P. de Rosnay, C. Tavolato, J.-N. Thépaut, F. Vitart, The ERA-Interim reanalysis: Configuration and performance of the data assimilation system. *Q. J. R. Meteorol. Soc.* **137**, 553–597 (2011).

47. T. Reichler, M. Dameris, R. Sausen, Determining the tropopause height from gridded data. *Geophys. Res. Lett.* **30**, 2042 (2003).

48. H. Hersbach, B. Bell, P. Berrisford, S. Hirahara, A. Horányi, J. Muñoz-Sabater, J. Nicolas, C. Peubey, R. Radu, D. Schepers, A. Simmons, C. Soci, S. Abdalla, X. Abellan, G. Balsamo, P. Bechtold, G. Biavati, J. Bidlot, M. Bonavita, G. De Chiara, P. Dahlgren, D. Dee, M. Diamantakis, R. Dragani, J. Flemming, R. Forbes, M. Fuentes, A. Geer, L. Haimberger, S. Healy, R. J. Hogan, E. Hólm, M. Janisková, S. Keeley, P. Laloyaux, P. Lopez, C. Lupu, G. Radnoti, P. de Rosnay, I. Rozum, F. Vamborg, S. Villaume, J.-N. Thépaut, The ERA5 global reanalysis. *Q. J. R. Meteorol. Soc.* **146**, 1999–2049 (2020).

49. T. Rieckh, B. Scherllin-Pirscher, F. Ladstädter, U. Foelsche, Characteristics of tropopause parameters as observed with GPS radio occultation. *Atmos. Meas. Tech.* **7**, 3947–3958 (2014).

50. B. Scherllin-Pirscher, A. K. Steiner, R. A. Anthes, M. J. Alexander, S. P. Alexander, R. Biondi, T. Birner, J. Kim, W. J. Randel, S.-W. Son, T. Tsuda, Z. Zeng, Tropical temperature variability in the UTLS: New insights from GPS radio occultation observations. *J. Climate* **34**, 2813–2838 (2021).

51. S.-W. Son, N. F. Tandon, L. M. Polvani, The fine-scale structure of the global tropopause derived from COSMIC GPS radio occultation measurements. *J. Geophys. Res.* **116**, D20113 (2011).

52. B. Angerer, F. Ladstädter, B. Scherllin-Pirscher, M. Schwaerz, A. K. Steiner, U. Foelsche, G. Kirchengast, Quality aspects of the Wegener Center multi-satellite GPS radio occultation record OPSv5.6. *Atmos. Meas. Tech.* **10**, 4845–4863 (2017).

53. A. K. Steiner, B. C. Lackner, F. Ladstädter, B. Scherllin-Pirscher, U. Foelsche, G. Kirchengast, GPS radio occultation for climate monitoring and change detection. *Radio Sci.* **46**, RS0D24 (2011).

54. A. K. Steiner, F. Ladstädter, C. O. Ao, H. Gleisner, S.-P. Ho, D. Hunt, T. Schmidt, U. Foelsche, G. Kirchengast, Y.-H. Kuo, K. B. Lauritsen, A. J. Mannucci, J. K. Nielsen, W. Schreiner, M. Schwärz, S. Sokolovskiy, S. Syndergaard, J. Wickert, Consistency and structural uncertainty of multi-mission GPS radio occultation records. *Atmos. Meas. Tech.* **13**, 2547–2575 (2020).

55. H. Wilhelmsen, F. Ladstädter, T. Schmidt, A. K. Steiner, Double tropopauses and the tropical belt connected to ENSO. *Geophys. Res. Lett.* **47**, e2020GL089027 (2020).

56. W. J. Randel, F. Wu, D. J. Gaffen, Interannual variability of the tropical tropopause derived from radiosonde data and NCEP reanalyses. *J. Geophys. Res.* **105**, 15509–15523 (2000).

57. G. Gu, R. F. Adler, Precipitation and temperature variations on the interannual time scale: Assessing the impact of ENSO and volcanic eruptions. *J. Climate* **24**, 2258–2270 (2011).

58. B. Scherllin-Pirscher, C. Deser, S. -P. Ho, C. Chou, W. J. Randel, Y. -H. Kuo, The vertical and spatial structure of ENSO in the upper troposphere and lower stratosphere from GPS radio occultation measurements. *Geophys. Res. Lett.* **39**, L20801 (2012).

59. H. Wilhelmsen, F. Ladstädter, B. Scherllin-Pirscher, A. K. Steiner, Atmospheric QBO and ENSO indices with high vertical resolution from GNSS radio occultation temperature measurements. *Atmos. Meas. Tech.* **11**, 1333–1346 (2018).

60. J. -P. Vernier, L. W. Thomason, J. -P. Pommereau, A. Bourassa, J. Pelon, A. Garnier, A. Hauchecorne, L. Blanot, C. Trepte, D. Degenstein, F. Vargas, Major influence of tropical volcanic eruptions on the stratospheric aerosol layer during the last decade. *Geophys. Res. Lett.* **38**, L12807 (2011).

61. K. Wolter, M. S. Timlin, El Nino/Southern Oscillation behaviour since 1871 as diagnosed in an extended multivariate ENSO index (MEI.ext). *Int. J. Climatol.* **31**, 1074–1087 (2011).

62. B. Naujokat, An update of the observed quasi-biennial oscillation of the stratospheric winds over the tropics. *J. Atmos. Sci.* **43**, 1873–1877 (1986).

63. M. Sato, J. E. Hansen, M. P. McCormick, J. B. Pollack, Stratospheric aerosol optical depths, 1850–1990. *J. Geophys. Res.* **98**, 22987–22994 (1993).

64. M. J. Mills, A. Schmidt, R. Easter, S. Solomon, D. E. Kinnison, S. J. Ghan, R. R. Neely III, D. R. Marsh, A. Conley, C. G. Bardeen, A. Gettelman, Global volcanic aerosol properties derived from emissions, 1990–2014, using CESM1(WACCM). *J. Geophys. Res. Atmos.* **121**, 2332–2348 (2016).

65. B. D. Santer, S. Solomon, G. Pallotta, C. Mears, S. Po-Chedley, Q. Fu, F. Wentz, C.-Z. Zou, J. Painter, I. Cvijanovic, C. Bonfils, Comparing tropospheric warming in climate models and satellite data. *J. Climate* **30**, 373–392 (2017).

66. B. D. Santer, S. Solomon, F. J. Wentz, Q. Fu, S. Po-Chedley, C. Mears, J. F. Painter, C. Bonfils, Tropospheric warming over the past two decades. *Sci. Rep.* **7**, 2336 (2017).

67. W. J. Randel, R. R. Garcia, N. Calvo, D. Marsh, ENSO influence on zonal mean temperature and ozone in the tropical lower stratosphere. *Geophys. Res. Lett.* **36**, L15822 (2009).